

MEMBRANE–WATER PARTITIONING, MEMBRANE PERMEABILITY, AND  
BASELINE TOXICITY OF THE PARASITICIDES IVERMECTIN,  
ALBENDAZOLE, AND MORANTELBEATE I. ESCHER,\*† CINDY BERGER,‡ NADINE BRAMAZ,† JUNG-HWAN KWON,† MANUELA RICHTER,†  
OKSANA TSINMAN,‡ and ALEX AVDEEF‡  
†Swiss Federal Institute of Aquatic Science and Technology, Eawag, 8600 Dübendorf, Switzerland  
‡PION, 5 Constitution Way, Woburn, Massachusetts 01801, USA

(Received 26 July 2007; Accepted 18 October 2007)

**Abstract**—A comparative hazard assessment of the antiparasitics ivermectin, albendazole, and morantel was performed, with a particular focus on bioavailability and uptake into biological membranes. The experimentally determined liposome–water distribution ratio at pH 7 ( $D_{lipw}$  (pH 7)) of the positively charged morantel was 100 L/kg lipid. The  $D_{lipw}$  (pH 7) of albendazole was 3,000 L/kg lipid. The membrane permeability determined with the parallel artificial membrane permeability assay was consistent with predictions from a quantitative structure–activity relationship (QSAR) for morantel but 14-fold lower than predicted for albendazole, which can be rationalized because neutral albendazole is, in fact, zwitterionic and the large dipole moment hinders permeation through hydrophobic membranes. An unusually large molecule, ivermectin was suspected to show decreased bioaccumulation because of its bulkiness, but experimental determination of solubility showed that it was 40-fold less soluble than expected from a QSAR between solubility and the octanol–water partition coefficient. In contrast, its membrane permeability appeared to be typical for a compound of the given hydrophobicity, but it was not possible to determine the membrane–water partition coefficient because of its low solubility and high affinity to the dialysis membrane of the experimental device. The  $D_{lipw}$  (pH 7) for ivermectin of 2,700 L/kg lipid was calculated with a QSAR model. Morantel and albendazole were baseline toxicants in the bioluminescence inhibition test with *Vibrio fischeri* and a test for inhibition of photosynthesis in green algae. Only ivermectin exhibited a specific effect toward algae, but the excess toxicity was not very pronounced and might be biased by the uncertainty of the estimated hydrophobicity descriptor. Overall, we did not find any unexpected effect on nontarget endpoints.

**Keywords**—Environmental risk assessment    Veterinary pharmaceuticals    Aquatic organism    Baseline toxicity  
Quantitative structure–activity relationship

## INTRODUCTION

The parasiticides albendazole, morantel, and ivermectin are used primarily to treat infections caused by helminths in cattle. They typically are administered through ingestion or injection and are partially excreted with feces. Parasiticides may pose an environmental hazard to dung organisms but also may be washed out from the dung into soil and surface water or photochemically or biologically degraded [1–3].

Ivermectin belongs to the group of avermectins. It is a semisynthetic product derived from a macrocyclic lactone produced by the soil actinomycete *Streptomyces avermitilis*, and it comprises a mixture of ivermectin B1a and B1b [4]. Besides its application for cattle, it also is used to treat river blindness in humans. The neurotoxicant ivermectin affects the nerve pulse transmission in various parasites via induction of chloride influx through interaction with the  $\gamma$ -aminobutyric acid receptor and the glutamate receptor [5]. Because it cannot cross the blood–brain barrier in mammals, it is less toxic to mammals but is highly toxic to a range of aquatic invertebrates, such as daphnids and shrimps, and even to fish, because it is assumed that it can pass the blood–brain barrier in fish [6,7]. Environmental risk assessments have concluded that a risk exists for dung organisms and, potentially, for soil organisms [1,8]. One study on the risk of ivermectin to marine organisms concluded that no risk exists for the marine environment in the vicinity of aquacultures [9].

The benzimidazole albendazole interferes with microtubule-dependent glucose uptake [5]. Albendazole is metabolized more extensively, but some of the excreted metabolites also have antiparasitic activity. Abundant literature exists regarding the environmental risk of ivermectin, but only few studies have been conducted with the benzimidazoles. Oh et al. [10] recently concluded that hazard quotients of various benzimidazoles, which were based on acute and chronic daphnia toxicity data, warrant further investigation of these anthelmintic agents [10].

Even less information is available for the pyrimidine morantel. It is poorly absorbed orally and, thus, is excreted in significant amounts with feces [11]. It was prioritized for environmental hazard assessment by Boxall et al. [12] and assigned to the same priority group as ivermectin. Morantel appears to be relatively harmless to dung fauna [13].

Despite the abundant literature, quite a few questions remain concerning the bioavailability and uptake of these three parasiticides. All three are nonclassical environmental pollutants. Ivermectin is a very large molecule, and previous bioaccumulation studies have suspected that membrane permeability ( $P_m$ ) is reduced because of the bulkiness of the molecule [14]. Consequently, uptake kinetics and calculated kinetic bioconcentration factors are smaller than expected for compounds of similar hydrophobicity.

Morantel is a base that is fully protonated and carries a positive charge at ambient pH values. In contrast, albendazole is neutral overall but, presumably, is zwitterionic. Charged molecules are expected to accumulate to a smaller extent into

\* To whom correspondence may be addressed (escher@eawag.ch).  
Published on the Web 11/27/2007.

aquatic organisms, because passive diffusion is energetically unfavorable and uptake models demonstrated that only the neutral species likely is taken up by passive diffusion and that the charged species will form only in the cytosol according to the acidity constant of the compound and the cytosolic pH [15]. Consequently, steady-state bioconcentration factors are lower than expected for corresponding neutral compounds. Overall partitioning of ionizable compounds into cells and biological organisms can be better predicted with the liposome–water distribution ratio at pH 7 ( $D_{lipw}$  (pH 7)) than with the octanol–water partition coefficient ( $K_{ow}$ ) of the neutral species or the ionization–corrected octanol–water distribution ratio at pH 7 [16]. Therefore,  $D_{lipw}$  (pH 7) was determined experimentally in the present study and used as an indicator to assess if the parasiticides act as baseline toxicants or according to a specific mode of action in the two investigated organisms, bacteria and algae.

Another indicator of the potential to bioaccumulate is the  $P_m$ . The parallel artificial membrane permeability assay (PAMPA) commonly is used as an in vitro model for passive uptake of pharmaceuticals in the gastrointestinal tract [17–19], but it recently was applied to mimic the passive absorption and elimination in small fish [20]. The measurement principle of PAMPA is as follows: A cocktail of membrane lipids dissolved in dodecane is spread on a porous membrane support, where a thin film membrane forms. This lipid membrane is then brought into contact with an aqueous phase containing the compound of interest on one side of the membrane (donor phase) and an aqueous phase devoid of the compound on the other side (acceptor phase). The increase of concentration in the acceptor phase is being measured as a function of time and the composition of the phases, and intrinsic permeability is derived from the experimental data as described by Avdeef [18]. The PAMPA gives information regarding the uptake kinetics and whether membrane permeation is possible, but at this point, the PAMPA cannot be used to estimate bioconcentration in aquatic organisms directly. For the parasiticides investigated here, the PAMPA experiments will be compared with the extended database on  $P_m$  measurements for drugs to explore if the nonclassical compounds, indeed, behave unexpectedly or obey the general principles of membrane permeation and partitioning.

We previously developed a mode of action–based battery of ecotoxicological test systems to evaluate primary mechanisms of toxicity and nontarget effects of human pharmaceuticals to aquatic life [21,22]. This test battery is comprised of five to eight in vitro, low-complexity test systems that cover a series of fundamental modes of toxic action plus a few particularly environmentally relevant receptor-mediated effects. This test battery was applied in the present study to check for potentially overlooked nontarget effects; therefore, none of the previously identified specific effects on aquatic and terrestrial invertebrates, such as dung flies and water fleas, were investigated again. In the present study, we tested for baseline toxicity, specific and nonspecific inhibition of photosynthesis, and receptor-mediated estrogenic, genotoxic, and other reactive mechanisms [21,22]. None of the results showed specific effects that would trigger more refined studies. We therefore focused the present study on two bioassays selected from this test battery, the 30-min bioluminescence inhibition test with the marine bacterium *Vibrio fischeri* and the 24-h chlorophyll fluorescence test with the green algae *Desmodesmus subspicatus*. Quantitative structure–activity relationships (QSARs)

of baseline toxicity are available for these two bioassays; therefore, it is possible to analyze if the nontarget effect of the parasiticides in these organisms can be explained by nonspecific membrane toxicity or if they are more toxic than predicted by baseline toxicity. The membrane affinity and permeability of the three parasiticides will be related to the toxic effects elicited in the two test systems. The focus of the analysis was the influence of the physicochemical properties of the investigated parasiticides on their bioavailability and effect.

With this focus, the present study makes a fundamental contribution to the hazard assessment of these compounds. It does not focus on the most sensitive invertebrate species but, rather, allows an improved interpretation of literature data regarding invertebrates (as demonstrated for the toxicity of ivermectin toward *Daphnia* sp. described below). The present study is only one of the puzzle pieces of the European Union Framework 6 project entitled “Environmental Risk Assessment of Pharmaceuticals” [23], in which ivermectin is one of the case-study chemicals and all environmental compartments as well as many other organisms are considered.

## MATERIALS AND METHODS

### Chemicals

The parasiticides ivermectin (Chemical Abstract Services [CAS] no. 70288-86-7; mixture of 94% ivermectin B1a and 2.8% ivermectin B1b), morantel (CAS no. 20574-50-9), and albendazole (CAS no. 959-24-0) were obtained from Sigma (Buchs, Switzerland). All buffers and medium components were purchased from Fluka (Buchs, Switzerland). Polyethylene glycol (PEG400) was obtained from VWR (Bridgeport, NJ, USA). Universal PRISMA<sup>™</sup> buffer (P/N 110151; pION, Woburn, MA, USA) was used for permeability determination.

### Chemical analysis

The concentrations of the parasiticides were quantified with high-performance liquid chromatography (HPLC) with a Summit HPLC System (Dionex, Olten, Switzerland) and ultraviolet detection (UVD 340-U; Dionex). A reversed-phase C18 column (length, 125 mm; inner diameter, 4 mm; film thickness, 5  $\mu$ m; Nucleodur Gravity; Macherey-Nagel, Oensingen, Switzerland) was used for separation. The eluent was composed of buffer (10 mM *ortho*-phosphoric acid and 2 mM 1-octanesulfonic acid at pH 5) and acetonitrile. The buffer to acetonitrile ratio was 55:45 for morantel, 50:50 for albendazole, and 30:70 for ivermectin. Compounds were detected at 230 nm (ivermectin), 315 nm (morantel), and 227 nm (albendazole).

### Physicochemical descriptors

Physicochemical descriptors were collected from different literature sources (see Table 1). Data gaps were filled experimentally using the methods described below.

### Acidity constant

The potentiometric acidity constant ( $pK_a$ ; Gemini<sup>™</sup>; pION) was used to determine ionization constants [24,25]. The  $pK_a$  of morantel was determined using 74 to 33% (w/w) methanol as cosolvent in six titrations with different methanol contents, followed by an extrapolation to 0% methanol.

### Solubility

The intrinsic solubility ( $S_0$ ) of albendazole and ivermectin were determined at  $25 \pm 3^\circ\text{C}$  using a  $\mu$ DISS Profiler<sup>™</sup> (pION),

Table 1. Physicochemical descriptors of the three parasiticides<sup>a</sup>

	pK <sub>a</sub>	f <sub>neutral</sub> (pH 7)	Log K <sub>ow</sub>	S <sub>0</sub> (mg/L)	C <sub>w</sub> <sup>sat</sup> (mg/L)	Log D <sub>lipw</sub> (pH 7)		P <sub>0</sub> (cm/s) <sup>c</sup>
						Predicted <sup>b</sup>	Experimental	
Morantel	11.91 <sup>d</sup>	3 × 10 <sup>-5</sup>	3.69 <sup>e</sup>	ND	423 ± 185 <sup>f</sup>	2.85	2.03	-2.05 ± 0.12
Albendazole	4.21/10.43 <sup>d</sup>	1.00 <sup>g</sup>	3.14 <sup>e</sup>	0.40 ± 0.02 <sup>h</sup>	0.42 ± 0.08 <sup>f</sup>	3.35	3.47	-3.12 ± 0.10
Ivermectin	Neutral	1.00	3.22 <sup>i</sup>	2.00 ± 0.05 <sup>h</sup>	0.72 ± 0.01	3.43	ND	-2.21 ± 0.08

<sup>a</sup> C<sub>w</sub><sup>sat</sup> = water solubility; f<sub>neutral</sub> = fraction of neutral species; K<sub>ow</sub> = octanol-water partition coefficient; ND = not determined; P<sub>0</sub> = intrinsic membrane permeability of the neutral species; S<sub>0</sub> = intrinsic solubility.

<sup>b</sup> Predicted from K<sub>ow</sub> and converted to liposome-water partition coefficient (K<sub>lipw</sub>), and then speciation was considered as described previously [22].

<sup>c</sup> Calculated from the experimental permeability data and the pK<sub>a</sub> of the compounds as described in *Materials and Methods*.

<sup>d</sup> Measured with pSol Gemini™ instrument (pION, Woburn, MA, USA), in presence of cosolvents, and extrapolated to aqueous pK<sub>a</sub>.

<sup>e</sup> Data from the Physprop database (<http://www.syrrs.com/esc/physprop.htm>).

<sup>f</sup> Solubility related to the molecular weight of the free base and zwitterions, not to the salt used in the experiment.

<sup>g</sup> Overall neutrality, but most likely in zwitterionic form.

<sup>h</sup> Solubility measured with μDISS Profiler™ (pION).

<sup>i</sup> Data from Bloom and Matheson [1] and Edwards et al [8].

<sup>j</sup> For ivermectin, solubility was determined independently by the modified shake flask method to be 4.11 ± 0.38 mg/L. ND = not determined.

which collects in situ concentration data in the presence of background solid. Compounds generally were introduced as a powdered sample, typically 0.2 to 0.5 mg in 3 ml of solubility medium in the six-vessel instrument. The PRISMA universal buffer, adjusted to pH 7.4 with 1 N NaOH and 18 MΩ deionized water, was used as the assay media. In all six vessels, ultraviolet spectra from 240 to 390 nm were collected. Solubility of the compounds was determined after 12 to 24 h, assuring that the dissolution profile reached saturation and an excess of the solid was present in the solution. The method requires no separation of the solid from the suspension to measure sample concentration.

For ivermectin, six dilution points in a concentration range from 0.6 to 10.0 mg/L were taken for the standard calibration curve. Then, approximately 0.2 to 0.5 mg of ivermectin was weighed into four test tubes of the μDISS Profiler. Three milliliters of deionized water (18 MΩ) were added. The stirring speed was set to 700 rpm. The concentration–time profile was calculated by the μDISS processing software (pION) based on the area under the second-derivative curves (optical density vs wavelength) in the wavelength interval from 260 to 268 nm, a strategy that minimizes the contributions from the background scattering of the turbid solutions.

The solubility of albendazole was measured, as described above, in 50 mM buffer solution adjusted to pH 7.4 with 1 N NaOH. In five vessels, the compound was introduced as a solid powder, and the dissolution profile was monitored over 17 h. Three microliters of 20 mM dimethyl sulfoxide (DMSO) solution of the compound were added to the sixth vessel. Final concentration of DMSO in the buffer was less than 1.0%.

Solubility also was determined using the miniaturized shake flask method [26]. In this method, filtration was used to separate solid from saturated solution. Residual DMSO concentration in the method [26] was kept at 1.0% (v/v) in the final buffer solutions.

#### Liposome–water partitioning

The D<sub>lipw</sub> (pH 7) values of albendazole and morantel were determined using the equilibrium dialysis method described by Escher et al. [27]. For determination of the D<sub>lipw</sub> (pH 7) of ivermectin, the recently developed ultracentrifugation method [28] also was used, because the majority of the compound was sorbed to the dialysis membrane and could not be recovered.

Small unilamellar liposomes were made from synthetic 1-palmitoyl-2-oleoyl-sn-glycero-3-phosphatidylcholine by the membrane extrusion method described by Kaiser and Escher [28]. Concentrations in the aqueous phase (C<sub>w</sub>) were determined by the HPLC method described above. The concentrations in the liposomes (C<sub>lip</sub>; mol/kg lipid) were computed by subtracting the C<sub>w</sub> in the reference dialysis cells without liposomes from the C<sub>w</sub> in the dialysis cells with liposomes, considering the liposome to water ratio [27]. The D<sub>lipw</sub> (pH 7) is defined as the ratio of C<sub>lip</sub> and C<sub>w</sub>. The D<sub>lipw</sub> (pH 7) values were derived from the slope of the linear regression of C<sub>lip</sub> as a function of C<sub>w</sub>, and the standard error of the slope was used to define the error of D<sub>lipw</sub> (pH 7).

#### PAMPA measurements

All PAMPA experiments were performed at 25 ± 3°C using the PAMPA evolution instruments from pION. The PAMPA 96-well sandwich was preloaded with 96 magnetic stirrers (PN 110212; pION). Morantel was introduced in the PAMPA assay as a citrate salt. Possible influence of the counterion on the

PRISMA buffer was studied using the simulation option of the  $pK_a$  Gemini Program (Ver 1.5; pION). Calculated results showed a shift of 0.1 pH unit from the required pH values. To avoid unwanted shift of pH in the donor compartment, quality control of the buffer was performed in the presence of morantel citrate at a concentration of 50  $\mu\text{M}$  (0.5%, v/v, DMSO in the background) at pH between 3 and 12. Permeability results for albendazole were taken from Avdeef [26].

The effective permeability ( $P_e$ ) of each compound was measured at pH between 3 and 12. The donor solutions were varied in pH (NaOH-treated PRISMA buffer), whereas the receiver solutions had pH 7.4 (gradient-pH sink). The buffers used in the donor were prepared automatically on Tecan Freedom Evo robotic system (Tecan, Männedorf, Switzerland). The quality control of the buffers and the pH electrode were performed by alkalimetric titration, incorporating the Avdeef-Bucher procedure [29]. Optimized pH-gradient conditions were selected, using the pOD procedure [18], to ensure that the pH would be above and below the  $pK_a^{\text{flux}}$  value (defined below) of the compounds. The pH variation was necessary to correct the  $P_e$  values for ionization and aqueous boundary layer (ABL) effects [18,30]. The receiver buffer solutions contained a surfactant mixture (lipophilic sink) to mimic some of the function of drug-binding proteins [31]. Vigorous stirring of the donor solutions was employed in the assay, with stirring speed set to produce an ABL thickness of approximately 40  $\mu\text{m}$  to match the ABL contribution of the measured  $P_e$  to that expected in the human gastrointestinal tract [30]. The PAMPA sandwich was assembled and allowed to incubate for 30 min for the highly permeable molecules in a controlled-environment chamber (Gut-Box<sup>TM</sup>, pION, PN 110205) with a built-in magnetic stirring mechanism. The sandwich was then separated, and both the donor and receiver wells were assayed for the amount of material present by comparison with the ultraviolet spectrum (230–500 nm) obtained from reference standard solutions. Mass balance was used to determine the amount of material remaining in the membrane filter and attached to the plastic walls of the microtiter plate [19].

The  $P_e$  value was calculated as described previously by Avdeef et al. [18] except that the filter area, 0.3  $\text{cm}^2$ , was multiplied by the apparent porosity, 0.76. This latter step ensured that the ABL thickness determined from PAMPA assays using filters with a different porosity would be on an absolute scale [31].

In the vicinity of organisms, the ABL thickness is expected to be from 10 to 100  $\mu\text{m}$  (e.g., 30  $\mu\text{m}$  for 1-g fish [20]), whereas in unstirred PAMPA, the ABL thickness can be as high as 4,000  $\mu\text{m}$  [29,30]. By taking stirred or unstirred PAMPA data over a range of pH values, it is possible to match the effect of the ABL to that expected in vivo by applying the so-called  $pK_a^{\text{flux}}$  method [18,30,32], in which  $P_e$  is related to  $P_m$  and the ABL permeability ( $P_{\text{ABL}}$ ) as shown in Equation 1:

$$\frac{1}{P_e} = \frac{1}{P_{\text{ABL}}} + \frac{1}{P_m} \quad (1)$$

where  $P_m$  is dependent on the pH of the bulk aqueous solution for acids and bases. The maximum possible  $P_m$  is designated  $P_0$ , the intrinsic permeability of the uncharged species. For monoprotic weak acids and bases, Equation 2 relates  $P_m$  to  $P_0$ :

$$\frac{1}{P_m} = \frac{10^{\pm(\text{pH}-pK_a)} + 1}{P_0} \quad (2)$$

with + used for acids and – used for bases. Other cases are

described elsewhere [18,33]. The logarithmic form of Equation 2 describes a hyperbolic curve, characterized by a horizontal region that indicates intrinsic permeability and a diagonal region with a slope of  $\pm 1$ . The bend of such curves corresponds to  $\text{pH} = pK_a$  of the molecule. Combining Equations 1 and 2 leads to Equation 3:

$$\frac{1}{P_e} = \frac{1}{P_{\text{ABL}}} + \frac{10^{\pm(\text{pH}-pK_a)} + 1}{P_0} \quad (3)$$

With highly permeable molecules, Equation 2 cannot be used to determine either  $pK_a$  or  $P_0$  because of the attenuation effect of the ABL, as indicated by Equation 3. Such ABL-limited transport is observed when  $P_0 \gg P_{\text{ABL}}$ . This generally is the case with lipophilic chemicals, for which the overall permeability is a property of water rather than of membrane and in which  $P_e$  typically is approximately  $30 \times 10^{-6}$  cm/s [30].

Because the direct  $pK_a^{\text{flux}}$  method cannot be used with low-solubility, nonionizable molecules, such as ivermectin, a cosolvent assay procedure, based on the Biomek-FX<sup>®</sup> ADMETox workstation (Beckman Coulter, Fullerton, CA, USA), was used. The PRISMA buffer at pH 7.4 with addition of 15, 20, 25, and 30% (v/v) PEG400 were used in the donor compartment to enhance the solubility of ivermectin. Aqueous permeability was extrapolated from cosolvent data.

#### Bioassays

All bioassays were performed as described by Escher et al. [21]. For assessing baseline toxicity and specific interference with the energy metabolism, we used the 30-min bioluminescence inhibition test with the marine bacterium *V. fischeri*. Direct and indirect effects on photosynthesis were evaluated with the 24-h chlorophyll fluorescence test with the green algae *D. subspicatus* using the chlorophyll fluorometer ToxY-PAM (Waltz, Effeltrich, Germany).

#### Mode-of-action analysis

The toxic ratio (TR; Eqn. 4) is defined as the quotient of the predicted median effective concentration (EC50) of the baseline toxicity of a given compound ( $\text{EC50}_{\text{baseline}}$ ) to the experimentally determined EC50 ( $\text{EC50}_{\text{experimental}}$ ) [34]. The TR allows differentiation between baseline toxicity and specific modes of action, with  $\text{TR} < 10$  pointing to baseline toxicity and  $\text{TR} \geq 10$  pointing to a specific mode of toxic action [34]:

$$\text{TR} = \frac{\text{EC50}_{\text{baseline}}}{\text{EC50}_{\text{experimental}}} \quad (4)$$

The QSAR to predict  $\text{EC50}_{\text{baseline}}$  for the 30-min bioluminescence inhibition test (Eqn. 5) and for the 24-h chlorophyll fluorescence assay (Eqn. 6) were determined earlier by Escher et al. [21]:

$$\log[1/\text{EC50}_{\text{baseline}}] (\text{M}) = 0.79 \cdot \log D_{\text{lipw}} (\text{pH } 7) + 1.54 \quad (5)$$

$$\log[1/\text{EC50}_{\text{baseline}}] (\text{M}) = 0.91 \cdot \log D_{\text{lipw}} (\text{pH } 7) + 1.10 \quad (6)$$

## RESULTS AND DISCUSSION

#### Acidity constants

The acidity constant  $K_a$  was determined with a  $pK_a$  Gemini instrument. The apparent  $pK_a$  in the presence of cosolvents were extrapolated to the aqueous  $pK_a$  by linear regression (data not shown). The resulting  $pK_a$  are listed in Table 1. Morantel is fully protonated, with a  $pK_a$  of 11.91, and at pH 7, it is

present in its cationic form. Albendazole has one  $pK_a$  value at 4.21 (deprotonation of the amine group) and the other one at 10.43 (protonation of the benzimidazole ring) and, therefore, is present as predominantly neutral overall but zwitterionic at pH 7 (dominant species calculated with the computer program SPARC [35]) (<http://ibmlc2.chem.uga.edu/sparc/>). Ivermectin does not possess any ionizable groups and is neutral.

#### Octanol–water partition coefficient

The log  $K_{OW}$  values of morantel and albendazole (Table 1) were taken from the Physprop database (<http://www.syrres.com/esc/physprop.htm>). Both are estimated values, not experimental values. The log  $K_{OW}$  value of ivermectin has been measured earlier [1,8]. All three  $K_{OW}$  values are in the same order of magnitude, between 1,000 and 3,000; thus, these compounds are not considered to be bioaccumulative.

#### Solubility

The  $S_0$  of the uncharged form was determined for albendazole with a  $\mu$ DISS profiler instrument and miniaturized flask shake method [26] (Fig. 1a). Solubility was 0.4 mg/L and more than doubled in the presence of 1% DMSO.

Figure 1b shows an averaged dissolution profile of ivermectin monitored over 17 h. The  $S_0$  of ivermectin was  $2.00 \pm 0.05$  mg/L, and just like that for albendazole, it doubled in the presence of 1% DMSO. Literature data regarding the solubility of ivermectin are scarce and inconclusive, ranging from 9 mg/L [4] to 4 mg/L [1], and the measured  $S_0$  is at the higher end of the reported literature data.

We did not measure the  $S_0$  of morantel, because it is positively charged at pH 7 and 7.4. Therefore, its solubility is not limiting in our tests. The apparent solubility in algal growth medium was 423 mg/L. The solubility of albendazole in algal medium was very similar to its  $S_0$  (Table 1). In contrast, we could dissolve 50% less ivermectin in the algal medium than was expected from  $S_0$ .

The solubility (Table 1) is lower than one would expect for compounds in this range of hydrophobicity, as can be demonstrated when applying the log  $S_0$ –log  $K_{OW}$  relationship given by Avdeef [19] (Eqn. 7):

$$\log S_0 \text{ (mol/L)} = -0.63 \cdot \log K_{OW} - 2.00 \quad (7)$$

If this equation is applied to albendazole, we get a log  $S_0$  of  $-3.98$ , whereas the experimental value is 108-fold lower. The same holds for ivermectin, for which the predicted solubility is 40-fold higher than the measured  $S_0$ , presumably because of the bulkiness of the molecule, which requires more water molecules to solubilize it. The comparison cannot be done for morantel, both because it is fully protonated and positively charged at pH 7 and because the apparent solubility is 30-fold higher than the predicted  $S_0$  of the neutral species.

#### Uptake in liposomal membranes

The  $D_{lipw}$  (pH 7) values are listed in Table 1. The experimental log  $D_{lipw}$  (pH 7) of the zwitterionic albendazole agrees very well with the prediction from the  $K_{OW}$  of this substance (computational method described by Escher et al. [22]) (Table 1). We use this QSAR model under the assumption that a zwitterion behaves as a neutral molecule. The good agreement between experimental and predicted values confirms the validity of this assumption.

The positively charged morantel has a lower affinity to the membrane than predicted from the QSAR model described

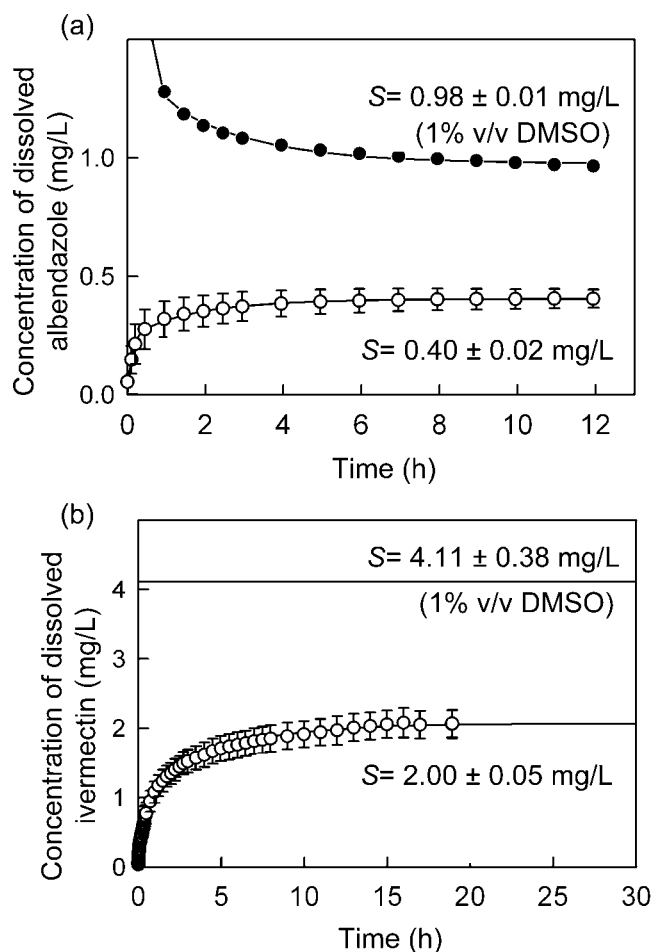


Fig. 1. Solubility ( $S$ ) measurements of (a) albendazole and (b) ivermectin at 25°C and pH 7.4. Black dots correspond to the data measured with the modified shake flask method [26] in the presence of 1% (v/v) dimethyl sulfoxide (DMSO), and open circles correspond to the data determined using the  $\mu$ DISS Profiler<sup>®</sup> (pION, Woburn, MA, USA) in the presence of background solid (powder). Error bars denote the standard deviations of the averages of six replicates.

above (Table 1), but the difference of less than one order of magnitude is well within the variability of the partition prediction model, in which we assume that the liposome–water distribution coefficient ( $K_{lipw}$ ) of the neutral species is 10-fold higher than that of the corresponding charged species. In fact, experimental  $K_{lipw}$  values for positively charged amines vary considerably, from being almost equal between the two corresponding species to a difference of two orders of magnitude (for a compilation of literature data, see Escher and Sigg [16]).

It was not possible to determine  $D_{lipw}$  (pH 7) for ivermectin. The equilibrium dialysis method did not work, presumably because a high fraction of ivermectin sorbed to the dialysis membrane. We could not confirm this assumption, because no mass balance could be measured. Alternatively, it is possible that the diffusion across the dialysis membrane is too slow for a high-molecular-weight compound like ivermectin. Size exclusion cannot be the cause, because the dialysis membrane has a cutoff of 10,000 Da. The porous diffusion coefficient, however, slows considerably with an increase in molecular weight. If we consider a porous membrane with a cutoff of 10,000 Da, like the one used here, then a compound with a molecular weight of 800 g/mol takes approximately 10-fold as long to diffuse through this porous membrane as compared

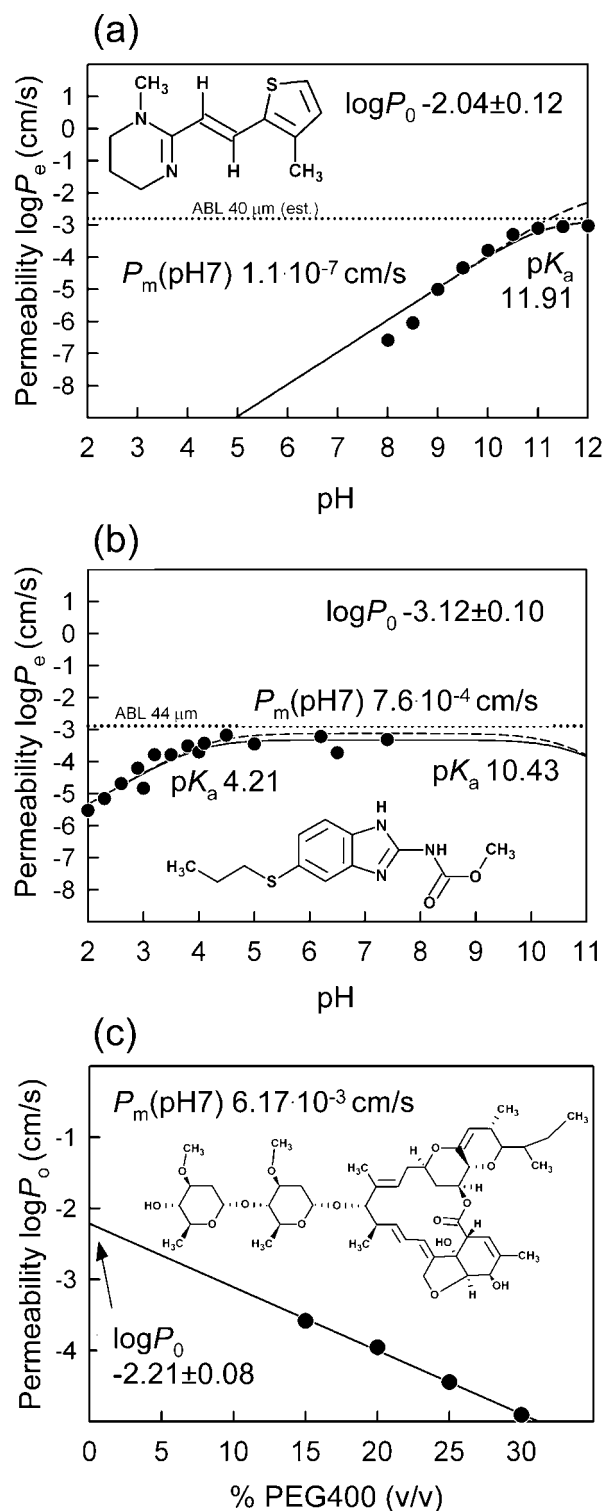


Fig. 2. Membrane permeability measurements of (a) morantel, (b) albendazole, and (c) ivermectin. **a.** The permeability ( $\log P_e$ ) of the base morantel was measured as a function of pH, and the intrinsic permeability ( $P_0$ ) was extrapolated from the slope of the pH-partition curve and the  $pK_a$  determined in separate experiments. Aqueous boundary layer (ABL) permeability ( $P_{ABL}$  in Eqn. 1) was estimated by the  $pK_a^{flux}$  method. Then, ABL thickness was estimated using the calculated aqueous diffusion coefficient of the solute. The estimated value was  $40 \mu\text{m}$ . **b.** The value was refined and converged to  $44 \mu\text{m}$ , indicating the estimation was very good. In addition, for albendazole, two  $pK_a$  values were considered. **c.**  $\log P_e$  of ivermectin was measured in presence of the cosolvent polyethylene glycol (PEG400), and the aqueous permeability  $P_0$  was determined by linear extrapolation to 0% PEG ( $r^2 = 0.997$ ,  $s = 0.039$ ).

to a compound with a molecular weight of  $200 \text{ g/mol}$  [36]. The ultracentrifugation method also produced artifacts. In many replicates of the experiments, we found highly variable but, on average, equal concentrations between the ultracentrifugation vials without and with liposomes, which were below the solubility limit determined above. Presumably, there occurs a colloidal agglomeration of ivermectin that is assigned to the soluble fraction after low-speed centrifugation but that actually precipitates in the ultracentrifuge. For the toxicity QSAR models, the predicted  $K_{lipw}$  ( $= D_{lipw}$  (pH 7) for the neutral ivermectin) was used.

#### Membrane permeability

Figure 2a and b shows the permeability profiles for morantel citrate and albendazole. The  $P_0$  of the neutral species of morantel (Fig. 2a) and albendazole (Fig. 2b) was deduced from plots of  $P_e$  as a function of pH at different stirring speeds (i.e., different ABL thicknesses). From these plots, it is possible to deduce  $P_0$  by extending the pH partition line to the measured  $pK_a$  as the inflection point.

Solid lines in Figure 2a and b indicate the best fit of the  $P_e$  values,  $\log P_e$  (filled circles), as a function of pH, according to the logarithmic form of Equation 3. The dashed-line  $P_m$  curves,  $\log P_m$  versus pH, result when the calculated ABLs (dotted horizontal lines) are factored out of the  $P_e$  values (Eqns. 1 and 2). The solid-line curve in Figure 2a is an example of ABL-limited transport, because at its maximum extent, it is substantially below the dashed-line curve. The permeability of albendazole (Fig. 2b) reflects the two macroscopic  $pK_a$  values of the amine at 4.21 (from positively charged to zwitterionic) and at 10.43 (from zwitterionic to negatively charged). Only the lower inflection point of the pH profile was used to deduce the intrinsic permeability of the neutral (zwitterionic) species. These extrapolated  $P_0$  values were  $8.91 \times 10^{-3} \text{ cm/s}$  for the neutral species of morantel and  $7.59 \times 10^{-4} \text{ cm/s}$  for the neutral species of albendazole.

The  $P_m$  of the neutral ivermectin was measured with PAM-PA in the presence of 15 to 40% PEG400 because of the solubility problems. The measured  $P_e$  lay in the range of  $8 \times 10^{-6} \text{ cm/s}$  (30% PEG400) to  $1.7 \times 10^{-4} \text{ cm/s}$  (15% PEG400) (Fig. 2c). A linear correlation of  $\log P_e$  as a function of the fraction of PEG400 allowed the linear extrapolation to pure water, and the corresponding  $P_0$  in aqueous solution was  $6.17 \times 10^{-3} \text{ cm/s}$  (Fig. 2c).

The experimentally obtained  $\log P_0$  values were compared with the QSAR prediction given by Equation 8, which was derived for a large compilation of 164 common drug molecules [19]. As expected,  $P_0$  increased with increasing lipophilicity, with a slope close to one, which means that an increase in hydrophobicity by a factor of 10 corresponds to the same increase in permeability:

$$\log P_0 (\text{cm/s}) = 1.18 \cdot \log K_{ow} - 5.68 \quad (8)$$

The predicted values of  $P_0$  (Fig. 3) were higher than the corresponding experimental values by a factor of 2.2 (ivermectin), 5.3 (morantel), and 14 (albendazole). The values for ivermectin and morantel lie well within the range of variability of the QSAR prediction [19]. The 14-fold lower experimental  $P_0$  of albendazole as compared to the QSAR prediction can be rationalized by the fact that albendazole actually is a zwitterion and that the permeability is expected to be hindered because of its relatively large dipole moment (6.2 Debye for the oxidized form of albendazole [37]).

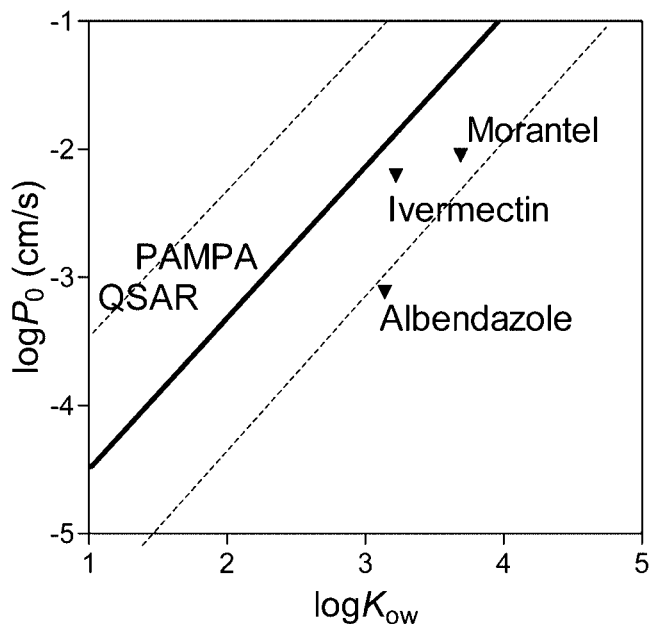


Fig. 3. Correlation of intrinsic membrane permeability of the neutral species ( $P_0$ ) as a function of the log octanol–water partition coefficient ( $K_{ow}$ ). Solid line corresponds to the quantitative structure–activity relationship (QSAR) regression line of the parallel artificial membrane permeability (PAMPA) measurements (Eqn. 8) [19], and dotted lines indicate the band of one order of magnitude higher and lower  $P_0$  values and experimental data from Table 1.

Because the  $P_m$  of ivermectin does not show any unusual behavior, we conclude that the inability to quantify the  $D_{lipw}$  (pH 7) is an experimental problem and not a result of negligible uptake. Therefore, we used the estimated  $D_{lipw}$  (pH 7) for the TR analysis reported below. Note, however, that the PAMPA membrane contains a large fraction of dodecane and, therefore, cannot perfectly mimic the steric constraints of biomembranes.

#### Consequences for bioconcentration in fish

Bioconcentration of ivermectin B1a was measured in bluegill sunfish [38] and in sturgeon [14]. In those studies, a bioconcentration factor 50-fold lower than expected from the  $K_{ow}$  was found because of an unusually low uptake rate. Van den Heuvel et al. [38] hypothesized that this unusual behavior resulted from steric constraints, because the large molecular dimension of  $17.0 \times 18.7 \times 18.4 \text{ \AA}$  surpasses the size-exclusion limits proposed by Opperhuizen et al. [39] for superlipophilic compounds.

The extremely low uptake rate constant in fish is not consistent with the experimental permeability obtained in the present study, although a PAMPA system was shown to be a good *in vitro* model to predict the uptake rate constant in fish [20]. The discrepancy may result from the low solubility of ivermectin reducing the available concentration for biological uptake. The assumption of size exclusion also may hold for ivermectin, however, because the PAMPA membranes contain a significant amount of dodecane, which does not form a highly organized structure as biomembranes.

#### Parasiticide stability under biotest conditions

Wislocki et al. [6] reported photolytic degradation of ivermectin B1 in sunlight with a decay half-time of less than 12 h. Therefore, we tested the stability of the investigated para-

siticides under the conditions of the biotests, some of which had to be conducted in the light.

The morantel concentration decreased by more than 60% during 24-h incubation in the light at  $260 \mu\text{E}/\text{m}^2/\text{s}$ . Additionally, an unknown substance appeared in the HPLC with a retention time of approximately 1 min before that of morantel. The degradation was not induced by light, because in the dark, some of the unknown degradation products were detected, albeit in smaller fractions. By optimizing the experimental conditions of the bioassay, we could reduce the formation of the degradation product to 2 to 10%, and we assumed that it contributed in a negligible way to the toxicity burden. This assumption can be rationalized as follows: With few exceptions, environmental degradation products and metabolites of drugs are of lower hydrophobicity, which is the case here because the retention of the unknown compound in the reverse-phase HPLC is lower than that of the parent compound. Unless a new toxicophore is formed and the transformation product shows a new specific mode of toxic action, which we assume to be unlikely based on structural analysis of the parent compound, the toxicity of the product also is lower by the same factor as the decreases in hydrophobicity [40].

On addition of algae in the dark, albendazole did not significantly change its dissolved concentration. After 24-h incubation in the light, however, 38 to 54% of albendazole had disappeared in the absence of algae and 24 to 42% in the presence of algae, pointing to photodegradation.

For ivermectin, we could not measure concentrations using HPLC if algae were added to concentrations below the solubility, presumably because of significant sorption to and uptake into the algae. Therefore, we determined the maximum concentrations in the presence of algae. In this situation, the concentration at saturation was  $0.69 \pm 0.12 \text{ mg/L}$ , which corresponds to that in the absence of algae ( $0.72 \pm 0.01 \text{ mg/L}$ ) (Table 1). Ivermectin appeared to be stable during 24-h incubation in the light at  $260 \mu\text{E}/\text{m}^2/\text{s}$ , because no significant difference was observed in the concentration in the dark and in the light as well as in the presence and absence of algae.

#### Bioluminescence inhibition test

In the bioluminescence inhibition test, albendazole and morantel showed a log-logistic concentration–effect curve (Fig. 4a). Albendazole reached only 50% effect up to the solubility limit, but it was possible to derive an  $EC_{50}$ . To obtain a fit at all, however, it was necessary to fit the concentration–effect curves with a constant slope of one. Knowing the exact slope is necessary if 5 or 10% effective concentrations are to be deduced from the concentration–effect curve. The  $EC_{50}$  is fairly robust, however, and is not much influenced by the slope, because it can be considered as an anchoring point for the concentration–effect curve. The resulting  $EC_{50}$ s are listed in Table 2. The  $EC_{50}$  for albendazole was 4.6 mg/L, which is fivefold less sensitive than the value reported by Oh et al. [10].

In contrast, up to the solubility limit, no significant effect of ivermectin could be measured (Fig. 4a). The highest concentration measurable using HPLC (after incubation and centrifugation of the bacteria) was  $0.24 \mu\text{M}$  ( $0.21 \text{ mg/L}$ ), which was slightly lower than the solubility limit in the algal medium. The maximum effect achieved at  $0.21 \text{ mg/L}$  was 25%, but scatter was large: At the same concentration, 0% effect also was measured. Tisler and Erzen [7] reported an  $EC_{50}$  of 0.69 mg/L for the 30-min bioluminescence inhibition test with *V. fischeri*.

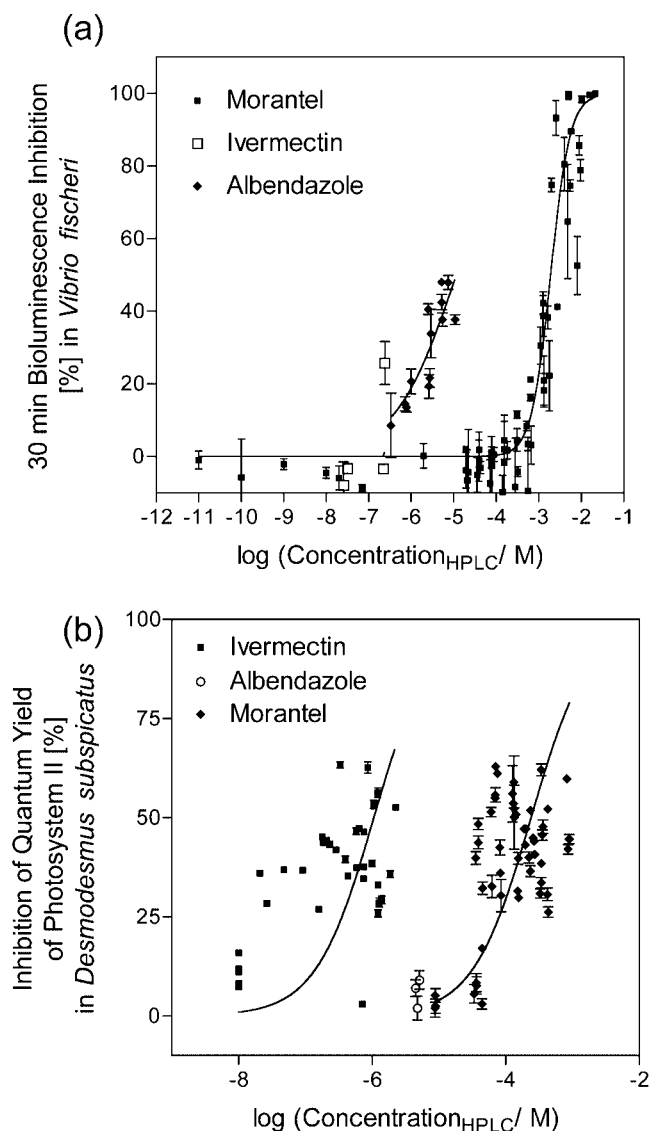


Fig. 4. Concentration–effect curves (a) in the bioluminescence inhibition test and (b) of inhibition of photosystem II (PS II) in the chlorophyll fluorescence test. The concentrations were verified in each test vial by high-performance liquid chromatography (HPLC).

When comparing the derived EC50s with QSARs for baseline toxicity (Eqn. 5), it is evident that albendazole and morantel act as baseline toxicants, with TRs (Eqn. 4) of 2.9 and 0.24, respectively. A deviation of the TR by a factor of three to four from the ideal TR of baseline toxicants can be considered as acceptable given the uncertainties in the QSAR, which was derived for neutral compounds and is now applied to charged species as well and given the experimental variability. Therefore,  $TR \leq 10$  typically is used as a criterion for

baseline toxicity [7]. No final conclusion can be drawn for ivermectin, because it was not soluble at the concentrations theoretically needed to elicit a baseline toxic effect (32 mg/L).

#### Chlorophyll fluorescence test

In the chlorophyll fluorescence test, a maximum effect of 60% for morantel and ivermectin was observed up to the solubility limit, but a maximum effect of less than 20% was observed for albendazole (Fig. 4b). Data variability was very large (see confidence intervals in Table 2), which results from all the uncertainty related to redissolution in the test vial, degradation in the light, HPLC analysis, and so on. Therefore, the concentration–effect curves were fitted with a constant slope of one, as was done for the bioluminescence inhibition test. Effect concentrations reported in Table 2 refer to analytically determined concentrations in each vial. The relatively large confidence intervals of the EC50s are related to the variability caused by the difficult test compounds. They are untypical for these bioassays, in which quality-control reference compounds 3,4-dichlorophenol for the bioluminescence inhibition test and diuron for the algal bioassay confirmed the reliability and quality of the bioassays [21,22]. Unlike studies by other authors, we did not increase solubility of the test compounds with cosolvent, because cosolvents interfere, in an undefined way, with bioavailability and toxicity (see the discussion above regarding the influence of cosolvent on solubility and permeability). In the present study, we added the test compounds in a solvent, evaporated the solvent by a gentle nitrogen stream, and redissolved the precipitated residue by test medium. Potential loss of the compound because of evaporation to dryness is accounted for by analyzing  $C_w$  at the end of each toxicity experiment in every test vial. This is a more rigorous procedure than typically applied but still has the uncertainty of slow dissolution kinetics, because  $C_w$  was determined in the test vial after the exposure and after centrifugation of the bio-material.

When comparing the EC50 to the predictions for baseline toxicity, it can be concluded that morantel and albendazole act as baseline toxicants whereas ivermectin has an excess toxicity with an estimated TR of more than 50 (Fig. 5). Given that the TR calculation was based on an estimated  $D_{ipw}$  (pH 7), this high TR does not allow the firm conclusion that ivermectin shows a specific effect in algae; it can only be taken as an indication.

The end point of photosystem II quantum yield after 24-h incubation (EC50, 0.94 mg/L) appears to be fivefold more sensitive than the 72-h chronic growth inhibition end point, which yielded an EC50 of 4.4 mg/L for *D. subspicatus* [7]. Additionally, *D. subspicatus* was more sensitive toward ivermectin than the green algae *Scenedesmus obliquus* and *Chlorella pyrenoidosa*, which had EC50s of 9.9 and 7.3 mg/L,

Table 2. Median effective concentrations (EC50s) of the investigated parasiticides<sup>a</sup>

	Bioluminescence inhibition test		Inhibition of photosystem II quantum yield	
	EC50 (μM)	EC50 (mg/L)	EC50 (μM)	EC50 (mg/L)
Morantel	1,910 (1,750–2,080)	506 (464–552)	239 (204–280)	63 (54–74)
Albendazole	11.1 (8.2–16.0)	4.6 (3.4–6.6)	>70	>30
Ivermectin	>0.2	>0.2	1.0 (0.8–1.3)	0.91 (0.73–1.13)

<sup>a</sup> Values in parentheses are the 95% confidence intervals.

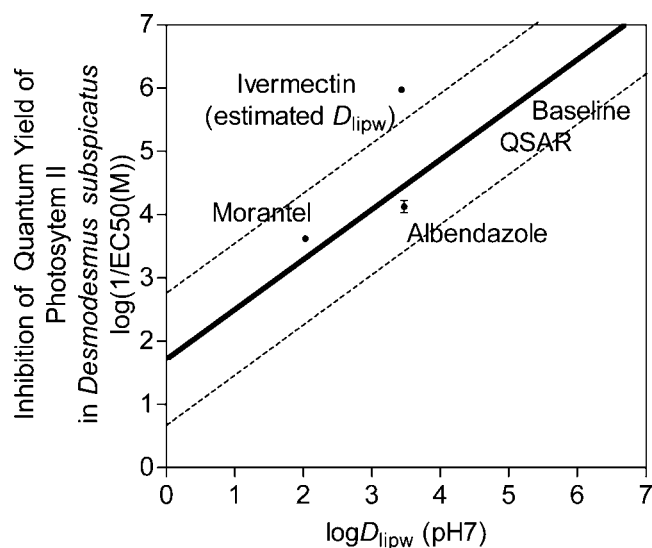


Fig. 5. Comparison of the median effective concentrations (EC<sub>50</sub>s) in the chlorophyll fluorescence test (dots) with predictions from the quantitative structure-activity relationship (QSAR) of baseline toxicity (drawn line; broken lines mark the baseline toxicity range of 0.1 < toxic ratio < 10). The EC<sub>50</sub> for albendazole is extrapolated from the limited available data; the liposome-water distribution ratio ( $D_{lipw}$  (pH 7)) of ivermectin is estimated.

respectively, in a 96-h growth inhibition test [41] despite the shorter exposure period.

#### Additional bioassays

The parasiticides were not active in the yeast estrogen screen, a selective test of receptor-mediated estrogenic activity. Ivermectin was tested in a concentration range from 1 nM to 1  $\mu$ M, morantel from 5 nM to 1 mM, and albendazole from 50 nM to 50  $\mu$ M. Even at the highest concentration, the induction was less than 5%, which was within the range of the variability of the negative control (evaporated ethanol). We also explored the effect of the parasiticides on the estrogenic effect of estradiol (i.e., a potential antiestrogenic effect). Compounds that affect the uptake of estradiol or its binding to the estrogen receptor have a quenching effect when an estradiol concentration that elicits an approximately 50% effect on its own is added to the assay. All parasiticides quenched the effect of estradiol by 10 to 30%. This effect was not dependent on concentration over six orders of magnitude, however, and the variability of effect was large. Therefore, we conclude that the parasiticides do not exhibit a direct antiestrogenic effect.

In the umu-Test for genotoxicity [21], ivermectin was tested in a concentration range from 1 nM to 1  $\mu$ M, morantel from 1 nM to 1 mM, and albendazole from 1 nM to 50  $\mu$ M. In all concentrations and both the absence and presence of activating S9 liver enzyme extract, no induction of the umuC DNA repair gene was observable. Also, growth of *Salmonella* sp. was not impaired in this concentration range. Thus, we can conclude that the test performed was valid but not positive.

#### CONCLUSION

Albendazole and morantel acted as baseline toxicants in all test systems investigated during the present study. Together with their relatively moderate hydrophobicity (accumulation in biological membranes at pH 7 by a factor of 100 for morantel and 3,000 for albendazole), one can conclude that they do not pose a hazard to the aquatic environment. The picture might

look different, however, if toxicity end points in target species are evaluated.

In contrast, for ivermectin, it is not possible to draw a clear conclusion. The large size of the molecule does not impair uptake by passive diffusion, but quantitative data are difficult to obtain because of experimental problems encountered when measuring partitioning into biological membranes. The estimated TR was greater than 10 in the algal chlorophyll fluorescence test. The estimation is based on a rather limited database, and the effect concentrations are extrapolations.

In conclusion, the three investigated parasiticides did not show any unexpected effect on nontarget organisms and end points. In target organisms (soil and aquatic invertebrates), however, the ecotoxicity can be quite dramatic. For example, the median lethal concentration of ivermectin toward daphnia is as low as 25 ng/L [1,42,43]. When comparing this value with the baseline toxicity QSAR for *Daphnia magna* [44] (reformulated to  $D_{lipw}$  (pH 7) as described by Escher and Schwarzenbach [45]), a TR of  $10^6$  is obtained, pointing to a very high specific toxicity for *D. magna*. Only the present results concerning membrane permeability and membrane-water distribution allow such a conclusion. Thus, a comprehensive risk assessment should focus on this and other sensitive end points, but the analysis should include the results for bioavailability and membrane-water partitioning presented here. The present, detailed study clearly shows that ivermectin in particular is a compound that is difficult to handle because of its low solubility, but it is not an unusual compound. Nevertheless, great care should be taken when handling ivermectin, and effect analysis always should be accompanied by a rigorous chemical analysis of the bioavailable concentration in the surrounding medium.

**Acknowledgement**—We thank Karen Duis. The present study was funded by the European Union under the 6th framework program in the project Environmental Risk Assessment of Pharmaceuticals (SSPI-CT-2003-511135) and by pION.

#### REFERENCES

- Bloom RA, Matheson JC. 1993. Environmental assessment of avermectins by the United States Food and Drug Administration. *Vet Parasitol* 48:281–294.
- McKellar QA. 1997. Ecotoxicology and residues of anthelmintic compounds. *Vet Parasitol* 72:413–426.
- Floate KD, Wardhaugh KG, Boxall ABA, Sherratt TN. 2005. Fecal residues of veterinary parasiticides: Nontarget effects in the pasture environment. *Annu Rev Entomol* 50:153–179.
- Campbell WC, ed. 1989. *Ivermectin and Abamectin*. Springer, New York, NY, USA.
- Martin RJ. 1997. Modes of action of anthelmintic drugs. *Vet J* 154:11–34.
- Wislocki PG, Grosso LS, Dybas RA. 1989. Environmental aspects of abamectin use in crop protection. In Campbell WC, ed, *Ivermectin and Abamectin*. Springer, New York, NY, USA, pp 182–200.
- Tisler T, Erzen NK. 2006. Abamectin in the aquatic environment. *Ecotoxicology* 15:495–502.
- Edwards CA, Atiyeh RM, Rombke J. 2001. Environmental impact of avermectins. *Rev Environ Contam Toxicol* 171:111–137.
- Davies IM, McHenry JG, Rae GH. 1997. Environmental risk from dissolved ivermectin to marine organisms. *Aquaculture* 158: 263–275.
- Oh SJ, Park J, Lee MJ, Park SY, Lee JH, Choi K. 2006. Ecological hazard assessment of major veterinary benzimidazoles: Acute and chronic toxicities to aquatic microbes and invertebrates. *Environ Toxicol Chem* 25:2221–2226.
- McKellar QA, Scott EW, Baxter P, Anderson LA, Bairden K. 1993. Pharmacodynamics, pharmacokinetics, and fecal persis-

- tence of morantel in cattle and goats. *J Vet Pharmacol Ther* 16: 87–92.
12. Boxall ABA, Fogg LA, Kay P, Blackwell PA, Pemberton EJ, Croxford A. 2003. Prioritization of veterinary medicines in the UK environment. *Toxicol Lett* 142:207–218.
  13. Lumaret JP, Errouissi F. 2002. Use of anthelmintics in herbivores and evaluation of risks for the nontarget fauna of pastures. *Vet Res* 33:547–562.
  14. Shen J, Ding S, Zhang S, Coats JR. 2005. Bioconcentration and elimination of avermectin B1 in sturgeon. *Environ Toxicol Chem* 24:396–399.
  15. Erickson RJ, McKim JM, Lien GJ, Hoffman AD, Batterman SL. 2006. Uptake and elimination of ionizable organic chemicals at fish gills: II. Observed and predicted effects of pH, alkalinity, and chemical properties. *Environ Toxicol Chem* 25:1522–1532.
  16. Escher BI, Sigg L. 2004. Chemical speciation of organics and of metals at biological interfaces. In Van Leeuwen HP, Köster W, eds, *Physicochemical Kinetics and Transport at Biointerfaces*, Vol 9. John Wiley, Chichester, UK, pp 205–271.
  17. Kansy M, Senner F, Gubernator F. 1998. Physicochemical high throughput screening: Parallel artificial membrane permeation assay in the description of passive absorption processes. *J Med Chem* 41:1007–1009.
  18. Avdeef A. 2003. *Absorption and Drug Development: Solubility, Permeability, and Charged State*. Wiley, Hoboken, NJ, USA.
  19. Avdeef A. 2006. High-throughput solubility, permeability, and the MAD PAMPA model. In Testa B, Krämer S, Wunderli-Alenspach H, Folkers G, eds, *Pharmacokinetic Profiling in Drug Research: Biological, Physicochemical, and Computational Strategies*. Verlag Helvetica Chimica Acta, Zürich, Switzerland, pp 221–243.
  20. Kwon J-H, Katz LE, Liljestrand HM. 2006. Use of a parallel artificial membrane system to evaluate passive absorption and elimination in small fish. *Environ Toxicol Chem* 25:3083–3092.
  21. Escher BI, Bramaz N, Eggen RIL, Richter M. 2005. In vitro assessment of modes of toxic action of pharmaceuticals in aquatic life. *Environ Sci Technol* 39:3090–3100.
  22. Escher BI, Bramaz N, Richter M, Lienert J. 2006. Comparative ecotoxicological hazard assessment of  $\beta$ -blockers and their human metabolites using a mode-of-action based test battery and a QSAR approach. *Environ Sci Technol* 40:7402–7408.
  23. Knacker T, Duis K, Ternes T, Fenner K, Escher B, Schmitt H, Römbke J, Garric J, Hutchinson T, Boxall ABA. 2005. The EU-project ERAPharm—Incentives for the further development of guidance documents? *Environ Sci Pollut Res Int* 12:62–65.
  24. Avdeef A. 1998. pH-metric solubility. 1. Solubility-pH profiles from Bjerrum plots. Gibbs buffer and  $pK_a$  in the solid state. *Pharm Pharmacol Commun* 4:165–178.
  25. Avdeef A, Berger CM, Brownell C. 2000. pH-Metric solubility. 2. Correlation between the acid-base titration and the saturation shake-flask solubility-pH methods. *Pharmacol Res* 17:85–89.
  26. Avdeef A, Bendels S, Tsinman KL, Kansy M. 2007. Solubility-excipient classification gradient maps. *Pharmacol Res* 24:530–545.
  27. Escher BI, Schwarzenbach RP, Westall JWC. 2000. Evaluation of liposome–water partitioning of organic acids and bases: I. Development of sorption model. *Environ Sci Technol* 34:3954–3961.
  28. Kaiser SM, Escher BI. 2006. The evaluation of liposome–water partitioning of 8-hydroxyquinolines and their copper complexes. *Environ Sci Technol* 40:1784–1791.
  29. Avdeef A, Nielsen PE, Tsinman O. 2004. PAMPA—A drug absorption in vitro model. 11. Matching the in vivo unstirred water layer thickness by individual-well stirring in microtiter plates. *Eur J Pharm Sci* 22:365–374.
  30. Avdeef A, Artursson P, Neuhoff S, Lazorova L, Gräsjö J, Tavelin S. 2005. Caco-2 permeability of weakly basic drugs predicted with the double-sink PAMPA  $pK_a^{flux}$  method. *Eur J Pharm Sci* 24:333–349.
  31. Nielsen PE, Avdeef A. 2004. PAMPA—A drug absorption in vitro model. 8. Apparent filter porosity and the unstirred water layer. *Eur J Pharm Sci* 22:33–41.
  32. Bendels S, Tsinman O, Wagner B, Lipp D, Parrilla I, Kansy M, Avdeef A. 2006. PAMPA-excipient classification gradient map. *Pharm Res* 23:2525–2535.
  33. Avdeef A. 2002. High-throughput measurements of permeability profiles. In van de Waterbeemd H, Lennernäs H, Artursson P, eds, *Drug Bioavailability Estimation of Solubility, Permeability, Absorption and Bioavailability*. Wiley-VCH, Weinheim, Germany, pp 46–71.
  34. Verhaar HJM, van Leeuwen CJ, Hermens JLM. 1992. Classifying environmental pollutants. 1: Structure–activity relationships for prediction of aquatic toxicity. *Chemosphere* 25:471–491.
  35. Hilal SH, Karickhoff SW, Carreira LA. 1995. A rigorous test for SPARC's chemical reactivity models: Estimation of more than 4,300 ionization  $pK_a$ s. *Quant Struct-Act Relat* 14:348–355.
  36. Renkin EM. 1954. Filtration, diffusion, and molecular sieving through porous cellulose membranes. *J Gen Physiol* 38:225–243.
  37. McCracken RO. 1990. Structure–activity relationships of benzothiazole and benzimidazole anthelmintics: A molecular modeling approach to in vivo drug efficacy. *J Parasitol* 76:853–864.
  38. Van den Heuvel WJA, Forbis AD, Halley BA, Ku CC, Jacob TA, Wislocki PG. 1996. Bioconcentration and depuration of avermectin B1a in the bluegill sunfish. *Environ Toxicol Chem* 15: 2263–2266.
  39. Opperhuizen A, van den Velde E, Gobas FAPC, Liem DAK, van den Steen JMD, Hutzinger O. 1985. Relationship between bioconcentration in fish and steric factors of hydrophobic chemicals. *Chemosphere* 14:1871–1896.
  40. Lienert J, Güdel K, Escher BI. 2007. Screening method for ecotoxicological hazard assessment of 42 pharmaceuticals considering human metabolism and excretory routes. *Environ Sci Technol* 41:4471–4478.
  41. Ma JY, Zheng RQ, Xu LG, Wang SF. 2002. Differential sensitivity of two green algae, *Scenedesmus obliquus* and *Chlorella pyrenoidosa*, to 12 pesticides. *Ecotoxicol Environ Saf* 52:57–61.
  42. Halley BA, Jacob TA, Lu AYH. 1989. The environmental impact of the use of ivermectin: Environmental effects and fate. *Chemosphere* 18:1543–1563.
  43. Halling-Sørensen B, Nors Nielsen S, Lanzky PF, Ingerslev F, Holten Lützhøft H, Jørgensen SE. 1998. Occurrence, fate, and effect of pharmaceutical substances in the environment—A review. *Chemosphere* 36:357–393.
  44. Zhao YT, Cronin MT, Dearden JC. 1998. Quantitative structure–activity relationships of chemicals acting by nonpolar narcosis—Theoretical considerations. *Quant Struct-Act Relat* 17:131–138.
  45. Escher B, Schwarzenbach RP. 2002. Mechanistic studies on baseline toxicity and uncoupling as a basis for modeling internal lethal concentrations in aquatic organisms. *Aquat Sci* 64:20–35.